Sensors and Actuators B 264 (2018) 27–37

Contents lists available at ScienceDirect

Sensors and Actuators B: Chemical

journal homepage: www.elsevier.com/locate/snb

Influence of mesoporous defect induced mixed-valent NiO (Ni^{2+}/Ni^{3+})-TiO_2 nanocomposite for non-enzymatic glucose biosensors

Saravanan Rajendran[a], Devaraj Manoj[b], Kumar Raju[c], Dionysios. D. Dionysiou[d], Mu. Naushad[e,*], F. Gracia[f,*], Lorena Cornejo[a], M.A. Gracia-Pinilla[g,h], Tansir Ahamad[e]

[a] Escuela Universitaria de Ingeniería Mecánica (EUDIM), Universidad de Tarapacá, Avda. General Velásquez 1775, Arica, Chile
[b] Department of Chemistry, School of Advanced Sciences, Vellore Institute of Technology, Vellore 632014, India
[c] Energy Materials, Materials Science and Manufacturing, Council for Scientific and Industrial Research (CSIR), Pretoria 0001, South Africa
[d] Environmental Engineering and Science Program, Department of Chemical and Environmental Engineering (ChEE), 705 Engineering Research Center, University of Cincinnati, USA
[e] Department of Chemistry, College of Science, Building#5, King Saud University, Riyadh, Saudi Arabia
[f] Department of Chemical Engineering, Biotechnology and Materials, University of Chile, Beauchef 851, 6th Floor, Santiago, Chile
[g] Universidad Autónoma de Nuevo León, Facultad de Ciencias Físico-Matemáticas, Av. Universidad, Cd. Universitaria, San Nicolás de los Garza, NL, Mexico
[h] Universidad Autónoma de Nuevo León, Centro de Investigación en Innovación y Desarrollo en Ingeniería y Tecnología, PIIT, Apodaca, NL, Mexico

ARTICLE INFO

Article history:
Received 30 November 2017
Received in revised form 13 February 2018
Accepted 23 February 2018
Available online 25 February 2018

Keywords:
Biosensor
Non-enzymatic
TiO_2
NiO
Modified electrode
Glucose

ABSTRACT

An extraordinary sensitive and selective non-enzymatic glucose sensor has been demonstrated based on the electrochemically highly stable NiO-TiO_2 mixed oxide comprising the defect induced mesoporous TiO_2 nanoparticles with Ni^{2+} and Ni^{3+} ions scattered on the surface. The defects on TiO_2 nanoparticles have been successfully introduced using NiO to investigate the interfacial properties between NiO and TiO_2. This defect induced interfacial behavior was characterized using X-ray diffraction, X-ray photoelectron spectroscopy and high-resolution transmission electron microscopy analyses. The obtained mixed oxide NiO-TiO_2 nanocomposite dispersion was drop casted on glassy carbon electrode to form a NiO-TiO_2/GCE modified electrode for non-enzymatic glucose sensor. The defects along with high surface area of mixed oxide enabled excellent electrocatalytic activity for glucose oxidation with sensitivity of 24.85 μA mM^{-1} cm^{-2} and detection limit of 0.7 μM (S/N = 3). The Ni ions scattered on the surface of TiO_2 nanoparticles, enabling effective charge transfer process, circumventing the agglomeration during prolonged detection, and resulting the unprecedented long-term stability and sensitivity. Thus, this defect induced mesoporous metal oxide nanocomposite is an outstanding candidate for application as redox active material in electrochemical biosensors.

1. Introduction

As indicated by the World Health Organization (WHO), diabetes will be the 7th leading cause of death and is projected to be double its value in the near future. Both Type I (insufficient insulin production) and Type II (incapability to use the insulin) diabetes need to be served sufficient insulin externally to avoid increase in the sugar level in the blood; otherwise failure to do this would lead to damage of the kidneys, eyes, and the nerves [1–4]. Indeed, there are several approaches that have been developed and commercialized sensors to monitor the glucose level in the blood [5,6]. However, non-enzymatic sensors allow glucose to be oxidized directly on the electrode surface and show superior sensing ability and stability compared to enzymatic counterparts as the latter develop thick enzymatic layer on their surface which prohibits the fast electron transfer. Moreover, the non-enzymatic glucose sensors have led to overcome number of limitations that enzymatic sensors have suffered including effects from the operating conditions such as temperature and humidity, and shorter lifetime due to denaturation of enzyme activity [7–10]. Therefore, numerous research studies have focused on the non-enzymatic glucose sensors, including those exploring the use of nanomaterials with engineered morphology because of their fast response time and operational stability, which in turn determine the long-term performance of the modified electrode.

Nanostructured titanium dioxide (TiO_2), a well-known metal oxide semiconductor, has gained significant attention due to its

* Corresponding authors.
E-mail addresses: mnaushad@ksu.edu.sa (Mu. Naushad), fgracia@ing.uchile.cl (F. Gracia).

https://doi.org/10.1016/j.snb.2018.02.165
0925-4005/

low cost, non-toxicity, biocompatibility, and high surface area with large number of active sites for various photocatalytic and electrochemical applications [11,12]. Apart from photocatalytic applications, numerous efforts have also been devoted towards the fabrication of nanostructured TiO_2 for other functions, including the synthesis of electrochemical sensors [13–15]. In general, the electrochemical properties of TiO_2 are strongly dependent on morphology, porosity, crystallinity, and dopant elements. Nevertheless, the utilization of pure TiO_2 in electrochemical applications as sensors has been limited because it hinders the fast electrochemical response towards analytes due to its wide bandgap (3.2 eV). Hence, to explore fast electrochemical response, TiO_2 based nanocomposites are selected as electrode platform in the present investigation.

The modification of electrodes with various redox-active metal oxides such as NiO, CuO and CoO is widely explored for non-enzymatic glucose sensing because the active metal center, especially when the oxide is available with large surface areas, generates more redox-active sites in alkaline medium which is critical for electrocatalytic reactions [16–18]. A few investigations have been carried out to explore the catalytic behavior of TiO_2 nanocomposites incorporating metal oxides for non-enzymatic glucose oxidation. Long et al. [19] studied the design of helical TiO_2 nanotube arrays modified with Cu_2O. Luo et al. modified the TiO_2 with CuO [20]. Yang et al. [21] reported the electrochemical deposition of Cu-Cu_2O based nanocomposites on TiO_2 surfaces. The resulting nanocomposite exhibited better analytical performance in presence of redox metal oxides when compared to pristine TiO_2 nanoparticles. Recently, Suneesh et al. [22] and Guo et al. [23] reported the enhanced electrochemical behavior of glucose oxidation by using Co-Cu alloy and Ni/CdS nanocomposites decorated TiO_2 nanotubes/nanowires, respectively. However, to exploit the electrocatalytic activity of TiO_2 based nanocomposites, the selection of dopant redox active metal oxide is of vital importance for glucose sensing.

Among the noble metal and transition metal oxides, NiO has received extensive attention as it has been recognized as an effective and inexpensive electrocatalyst. However, NiO-based non-enzymatic glucose sensors have low durability due to gradual detachment and dissolution of the catalyst from the substrate. In this respect, many studies have recently been focused on the modification of NiO with different substrate materials such as graphene, SiC, and TiO_2 nanostructures to ascertain long-term stability [24–26]. Though the latter materials have extended the stability to some extent compared to pure NiO, they still possess relatively low sensitivity and insufficient stability because of agglomeration of particles on the substrate surface. Consequently, the present work aims at improving the selectivity and long-term stability of non-enzymatic glucose sensor by fabricating NiO-TiO_2 on glassy carbon electrode (GCE). In this work, for the first time, we have synthesized defect induced mesoporous (Ni^{2+}/Ni^{3+})-TiO_2 nanocomposite by combined sol-gel method and thermal decomposition via vapor to solid route to overcome the possible particle agglomeration and dissolution of NiO for prolonged glucose oxidation.

2. Experimental section

2.1. Chemicals and materials

Titanium tetra isopropoxide (TTIP), isopropyl alcohol, citric acid, and nickel acetate were purchased from Sigma-Aldrich. D-Glucose and sodium hydroxide were received from Sisco Research Laboratories, India. All other reagents and solvents were of analytical grade and used as received unless otherwise specified. For electrochemical measurements, the supporting electrolyte of 0.1 M was prepared using NaOH. All solutions used in the experiments were prepared with Milli-Q water.

2.2. Preparation of mesoporous TiO_2 nanoparticles

The colloidal mixtures were prepared through 30 mL of TTIP solution dissolved in 150 mL of isopropyl alcohol (1:5 ratio) under continuous stirring condition at 600 rpm. An aqueous solution containing 0.5 M citric acid was slowly added into the colloidal mixture, and allowed to stir continuously for few minutes until it became in gel form. The obtained white gel was dried at 150 °C for 30 min to form a pre-synthesized TiO_2 powder. Finally, the pre-synthesized TiO_2 powder was calcined at 450 °C for 1 h to provide mesoporous TiO_2 nanoparticles.

2.3. Preparation of mesoporous NiO-TiO_2 nanocomposite particles

A required amount of pre-synthesized TiO_2 powder (obtained from previous step) was ground with nickel acetate (9:1) mixture for ~3 h using agate pestle and mortar. The powder raw mixture was calcined in a muffle furnace at 450 °C for 1 h. During this heating process, the mixed raw materials were slowly decomposed and thus the water and acetate content vaporized. After cooling down, the vaporized particles slowly condensed in a crucible (substrate), hence the defects on the surface of the crucible (substrate) served as locations for nucleation of the oxide vapors [27]. Further cooling to room temperature, the condensation process allowed such nuclei to grow into mesoporous NiO-TiO_2 nanoparticles. The obtained NiO-TiO_2 nanoparticles were examined by X-ray fluorescence (XRF) and the results revealed that TiO_2 and NiO nanoparticles co-existed as 95.5:4.5 ratio in the prepared mesoporous NiO-TiO_2 nanocomposite.

2.4. Instrumentation

X-ray diffractometer (XRD, D5000 diffractometer, Siemens, USA) with $CuK_{\alpha 1}$ ($\lambda = 1.5406$ Å) radiation and operated at 40 kV and 30 mA was employed to determine the crystalline nature and structure of the materials. The hybrid structure and morphology of the materials were examined using a high-resolution transmission electron microscope (HR-TEM), using FEI TITAN G2 80-300 (operated at 300 keV) along with EDS. The chemical composition of the samples was analyzed using X-ray fluorescence (XRF, EDX-720, Shimadzu). X-ray photoelectron spectroscopy (XPS) analysis using a Thermo Scientific Escalab 250Xi instrument was performed to determine the oxidation state of the prepared materials. The mesoporosity and the specific surface area of the materials were calculated using the BET equation on adsorption-desorption data obtained from a Micromeritics ASAP 2020 (USA) porosimeter. The electrochemical experiments were performed using CHI760E electrochemical workstation (CH Instruments, Austin, Texas). All the electrochemical measurements were carried out with a conventional three electrode system using glassy carbon electrode (GCE) of 3 mm diameter with 0.0707 cm^2 geometric area as working electrode, a platinum coil as the auxiliary electrode, and saturated Ag/AgCl (3 M KCl) as the reference electrode against which all potentials in this paper are reported.

2.5. Fabrication of NiO-TiO_2/GCE

Initially, GCE surface was carefully polished with increasing grades of alumina powder (1.0, 0.3 and 0.05 μm) and then it was further cleaned ultrasonically with ethanol and Milli-Q water mixture (1:1) to remove the traces of alumina and other contaminants. Subsequently, 10 μL of NiO-TiO_2 dispersion (1 mg/200 μL in

ethanol) was drop-cast on the pre-cleaned GCE surface and allowed to dry in air under ambient conditions. After drying, the NiO-TiO_2/GCE modified electrode was washed with water and finally dried under N_2 stream. For comparison, NiO/GCE and TiO_2/GCE electrodes were also prepared by adopting similar fabrication procedures to compare the electrochemical performance towards glucose.

3. Results and discussion

In this study, the new combination of sol-gel and thermal decomposition methods was utilized to prepare the defect induced NiO-TiO_2 nanocomposite by vapor to a solid mechanism. The prepared mesoporous material was examined by different characterization techniques to identify the particle composition, structure, shape, phase, and size of the composite material.

The formation of phase purity and structure of the pure TiO_2 and defect induced NiO-TiO_2 (Ni^{2+}/Ni^{3+}) mixed oxide materials were examined by XRD analysis and their corresponding diffraction peaks are presented in Fig. 1(a). The entire diffraction spectrum of pure TiO_2 was scrutinized by TOPAS Rietveld refinement and the details are in supporting information (Fig. SI 1). The refinement results show that the prepared pure TiO_2 exhibits anatase tetragonal structure with a goodness of fit (GOF) value of 1.26. The calculated crystallite size for TiO_2 is 18.1 nm and the lattice parameter values with a = 3.791 Å and c = 9.508 Å; the diffraction spectrum of TiO_2 is well matched with JCPDS card no: 21-1272.

The accumulation of NiO into TiO_2 material does not affect the anatase tetragonal structure of TiO_2. However, a new peak is present at 2θ of 43.18° which is highlighted in Fig. 1(a). This peak corresponds to 200 plane of cubic NiO material (JCPDS No: 47-1049). The refinement results (Supporting Information-Fig. SI 2) reveal the formation of mixed structures and their lattice parameter values show the presence of tetragonal TiO_2 (a = 3.797 Å and c = 9.522 Å) along with cubic NiO (a = 4.190 Å) with a GOF of 1.30. Further, the refinement results specify that a small amount of amorphous material exists in this mixed material. As shown in Fig. 1b, the major diffraction peak of 101 plane at 2θ = 25.28° of NiO-TiO_2 mixed oxide exhibits more broadening and slightly diverges into the higher angle than pristine TiO_2 (2θ = 25.11°). This suggests that many interfaces exist in the mixed structure due to the distribution of Ni^{2+} (0.72 Å) ions into the Ti^{4+} (0.68 Å) surfaces [28–30]. The crystallite sizes were calculated to be 18.2 nm for TiO_2 and 7.3 nm for NiO in the mixed system. Hence, the XRD results confirmed that the prepared nanocomposite material possesses hybrid structure.

The chemical composition and oxidation states of species in the prepared hybrid oxide material were studied by XPS. Fig. 2(a) shows the survey spectrum of the synthesized mixed oxide sample revealing the presence of Ti, Ni, O and C elements. The HR-XPS (Fig. 2(b)) shows two prominent Ti $2p_{3/2}$ and Ti $2p_{1/2}$ peaks at 462.4 eV and 456.7 eV with the energy difference of 5.7 eV. The results show that the peaks at 463.7 and 458.0 eV are shifted to lower binding energies in comparison with pristine TiO_2 nanoparticles (Supporting Information-Fig. SI 3). Because the NiO nanoparticles are well distributed on the TiO_2 surface or create some defects in TiO_2 in the mixed system, this enhances surface unsaturation which leads to lowering the binding energies. This is in agreement with the previous reports [31–35]. The deconvoluted HR-XPS peaks of Ni $2p_{3/2}$ and Ni $2p_{1/2}$ are shown in Fig. 2(c). The binding energies of Ni peaks indicate that the integrated peaks split into Ni^{2+}, Ni^{3+} and coexist with Shirley shake up or satellite peaks. This observation suggests that surface unsaturation properties lead to formation of both defects and more interface between NiO and TiO_2 materials, which lead to the formation of amorphous Ni_2O_3. In such case, it is more favorable to promote Ni^{3+} ions into the mixed states [31,36]. As illustrated in Fig. 2(d), the deconvoluted spectrum of O 1 s in the mixed oxide evidences the four fragmented oxygen peaks at 529.2, 529.8, 530.9 and 531.3 eV. The predominant peak observed at 529.2 eV is attributed to Ti^{4+} ions; the oxygen peak at 529.8 eV is attributed to surface hydroxyl, while the peaks at 530.9 and 531.3 eV are attributed to oxygen bonded with Ni^{2+} and Ni^{3+}, respectively [31–36]. Therefore, the XPS spectra confirm that the synthesized sample contains Ti^{4+}, Ni^{3+}, and Ni^{2+} ions.

The presence of defects in the mixed structure and its interface was investigated by TEM, HAADF, SAED and HR-TEM analyses. The TEM image of the prepared NiO-TiO_2 is shown in Fig. 3a. The image visibly indicates the presence of large spherical shaped TiO_2 nanoparticles with an average diameter around ~18 nm along with small NiO spherical particles and within the size between 6–8 nm. The small shaped NiO particles are well scattered on the TiO_2 surface rather than being segregated or decorated and therefore the samples possess mesoporous nature which was confirmed by HAADF (Fig. 3b) image. These effective interfaces and the uniform scattering of NiO nanoparticles had altered the electronic structure and the surface interfaces of NiO-TiO_2 mixed oxide [36–41]. The SAED pattern (Fig. 3c) of the prepared NiO-TiO_2 visualizes that there are numerous electron diffraction rings. The ring pattern was indexed with calculated d-spacing values and their consistent *hkl* planes are denoted in the image. The outcome was matched with the tetragonal structure of TiO_2 (JCPDS No: 71-1167) and cubic structure of NiO material (JCPDS No: 75-0197).

The HR-TEM image of prepared NiO-TiO_2 material shows more line dislocation or linear defect which is highlighted by the circle mark as displayed in Fig. 3d. During the synthesis of NiO-TiO_2, the condensation process between NiO and TiO_2 stimulates the surface unsaturation leading to more defects on the material. [36–41]. The d-spacing values obtained from the HR-TEM (Fig. 3e) confirm the tetragonal structure of anatase TiO_2 with corresponding lattice plane (004), and cubic NiO with (200) and (111) planes. It is clearly seen that the close surveillance of the HR-TEM images (Fig. 3e & f) revealed unclear edges which corresponds to the amorphous region of particles. The corresponding selected area electron diffraction (SAED) pattern (Fig. 3g) also confirms the presence of amorphous portion. Besides, the unclear or amorphous portion obtained from the HR-TEM images represents Ni^{3+} state in the mixed oxide and a similar argument has been made in accordance with the results obtained by XRD and XPS analyses. Hence, the as-prepared mixed oxide (NiO-TiO_2) material contains both line defects and amorphous nickel oxide in the form of Ni^{3+} and Ni^{2+} ions.

Textural properties such as pore volume, pore size, and specific surface area of the synthesized materials were determined by BJH and BET methods. As depicted in Fig. 4, the resulted nitrogen (N_2) adsorption-desorption isotherm of the mixed oxide directs H3 type hysteresis pattern. The surface parameters of prepared pure and mixed oxide materials are presented in supporting information (Table SI 4). When compared with the pure system, the mixed oxide material shows large pores which were formed due to the thermal decomposition of the raw materials. In other words, the condensation followed by the nucleation processes during thermal decomposition induced the mesoporosity on the surface of NiO-TiO_2 [42,43]. Navarro et al. stated that growth of novel phase metal oxides with low molecular volume takes place during thermal decomposition route. This permits the development of mesoporous materials; for example, the transformation of calcite to mesoporous CaO is achieved by this method [43].

3.1. Electrochemical characterization of the modified electrode

To compare the conductivity and interface properties of the modified GCE obtained by drop casting of NiO-TiO_2, pure NiO and TiO_2 dispersion on the GCE surface at different steps during fabrica-

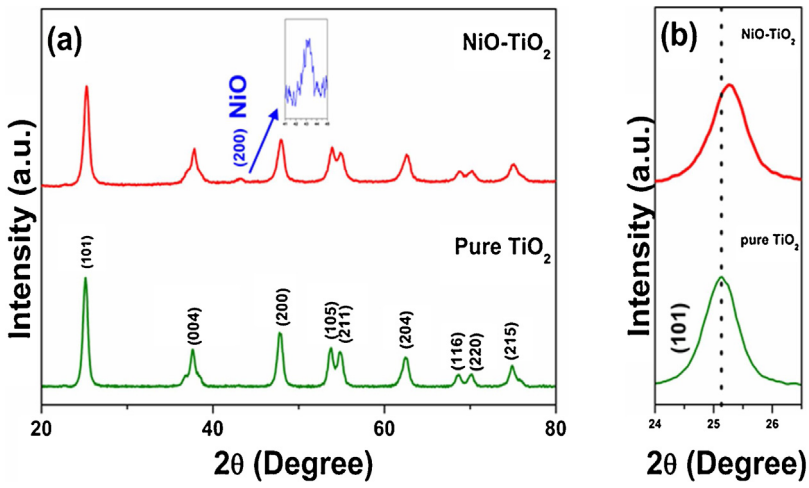

Fig. 1. (a) XRD patterns of the prepared materials and (b) major diffraction (101) peak of TiO_2 in the prepared materials.

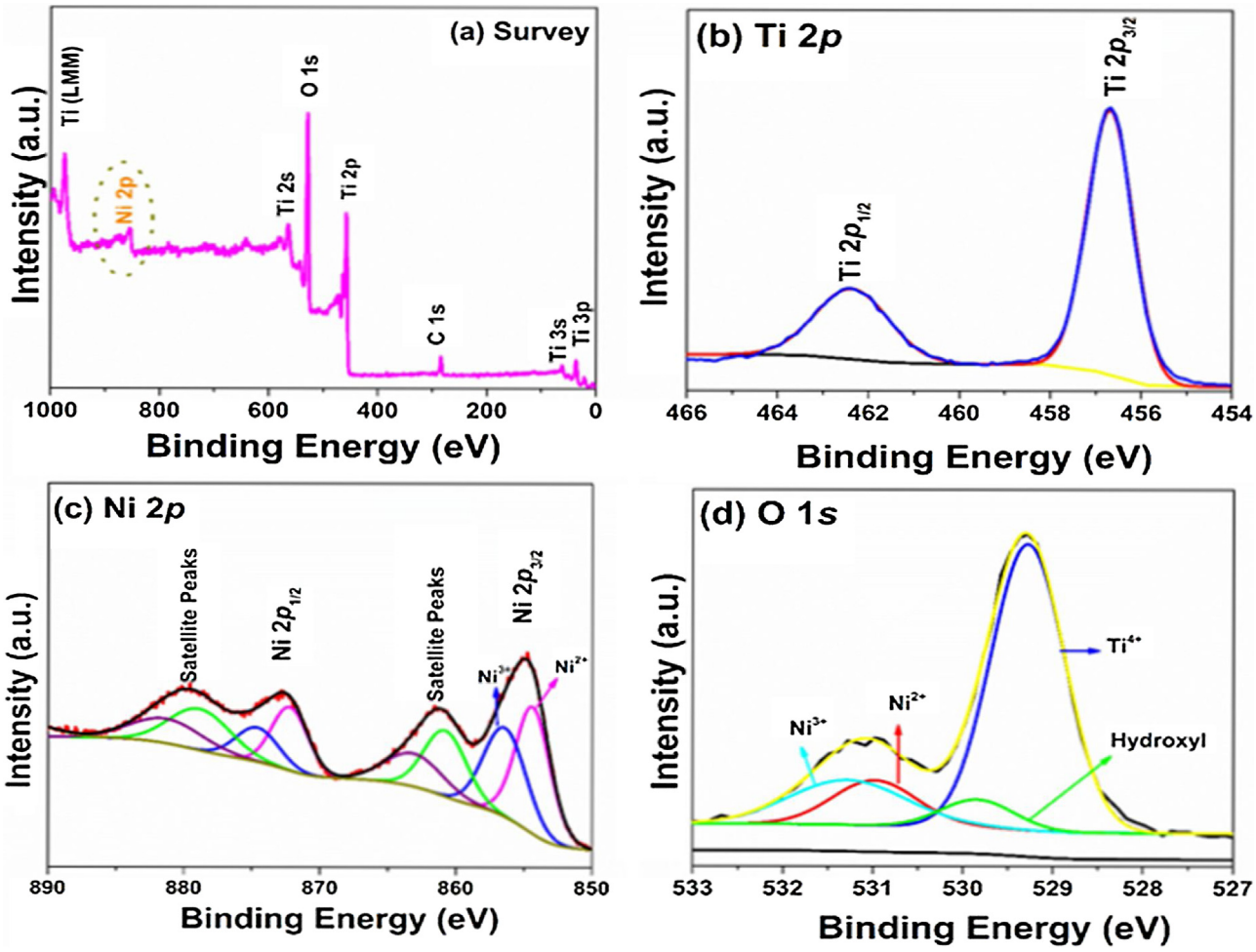

Fig. 2. XPS spectrum of the prepared NiO-TiO_2 mixed oxide material (a) survey, (b) Ti 2*p*, (c) Ni 2*p*, and (d) O 1*s*.

tion, we employed electrochemical impedance spectroscopy (EIS) in presence of 2 mM $[Fe(CN)_6]^{3/4-}$ containing 0.1 M KCl. In general, the Nyquist plot shows a large semicircle at the higher frequencies and a straight line at lower frequencies corresponding to electron transfer limited and diffusion controlled electrochemical processes, respectively. The charge transfer resistance (Rct) is calculated from the diameter of the semicircle observed from higher frequencies. As observed from Fig. 5a, TiO_2/GCE exhibits a larger Rct (2185 Ω), suggesting that the presence of TiO_2 nanostructures on modified GCE hinders the electron transfer between the redox probe and the electrode surface due to the high semi-conducing properties of TiO_2. On the contrary, the NiO/TiO_2 on the modified GC shows the lowest Rct value (1371 Ω) with an evidence of smaller semicircle diameter than that of bare GC (2062 Ω) and NiO coated GC (1852 Ω). Indeed, the formation of defects on the TiO_2 surface by NiO significantly improves the surface properties between TiO_2 and NiO, and

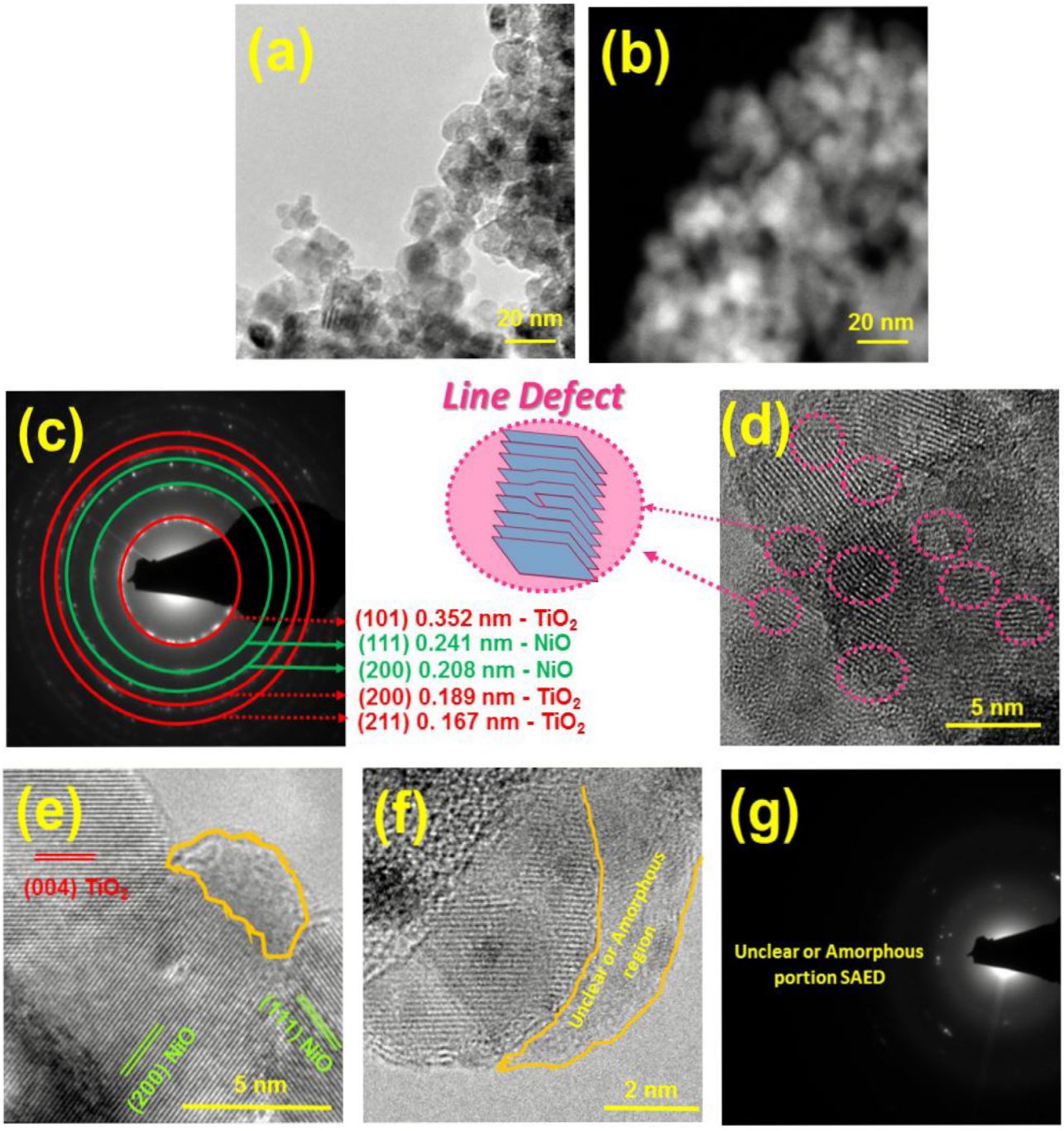

Fig. 3. (a) TEM spectrum of the prepared NiO-TiO_2 mixed oxide material, (b) HAADF image, (c) SAED of the polycrystalline region, (d–f) HR-TEM images and (g) SAED of unclear or amorphous region.

thus enabling rapid transport of electrons to the electrode surface, which in turn results in decent redox behavior when compared with pure TiO_2 system.

The electrochemical performance of these different modified electrodes were investigated by cyclic voltammetry (CV) in presence of 0.1 M NaOH at a scan rate of 50 mV s^{-1} and the results are presented in Fig. 5b. The electrochemical response for both bare GCE and TiO_2/GCE did not display any inherent redox response due to the absence of redox active species. It is interesting to note that the mesoporous NiO-TiO_2/GCE has shown a pair of well-defined quasi-reversible redox peaks with Epa = 0.489 V; Epc = 0.405 V and peak-peak separation (ΔEp) of 84 mV, which are assigned to Ni^{3+}/Ni^{2+} redox couple in presence of NaOH electrolyte. For comparison, NiO nanoparticles cast over GC were also subjected to cyclic voltammetry analysis and the corresponding voltammogram shows a pair of redox peaks with Epa = 0.462 V; Epc = 0.357 V and ΔEp = 105 mV.

The appearance of well-resolved quasi-reversible redox peaks for both NiO/GCE and NiO-TiO/GCE is due to the surface oxidation of NiO to $Ni(OH)_2$, followed by further oxidation to NiOOH. This results in the occurrence of faradaic reactions between NiOx/Ni(OH)x and NiOOH at the electrode surface. Unlike other modified electrodes studied, the NiO-TiO_2/GCE shows higher peak current response and less peak-peak separation. These results indicate the defect-induced mesoporous TiO_2 avails more number of accessible active sites for fast electron transfer.

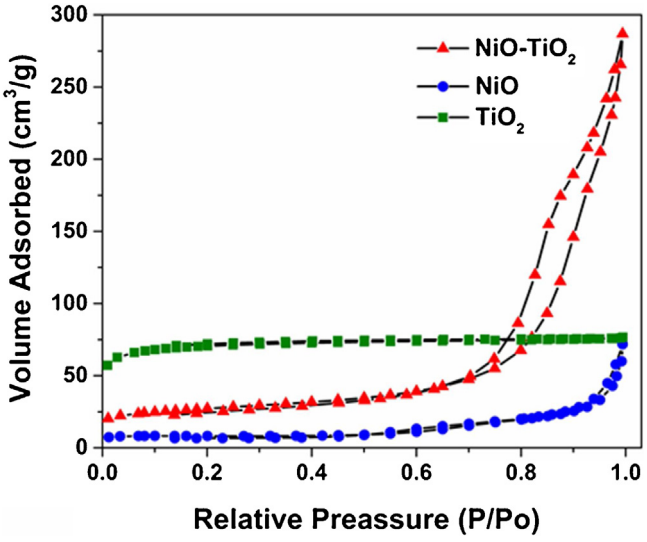

Fig. 4. Nitrogen adsorption-desorption isotherm of the prepared materials.

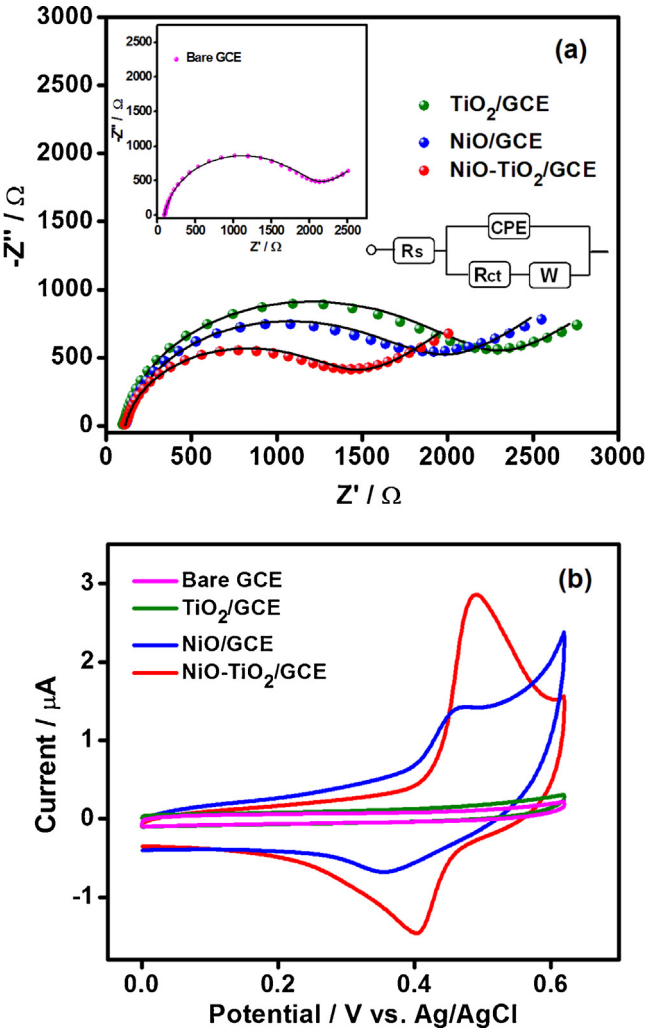

Fig. 5. (a) Nyquist plot of TiO_2/GCE, NiO/GCE and NiO-TiO_2/GCE modified electrodes recorded in presence of 2 mM $[Fe(CN)_6]^{3-/4-}$ containing 0.1 M KCl electrolyte. The EIS response for bare GCE is represented as inset. (b) CVs for bare GCE, TiO_2/GCE, NiO/GCE and NiO-TiO_2/GCE in presence of 0.1 M NaOH at 50 mV s^{-1}.

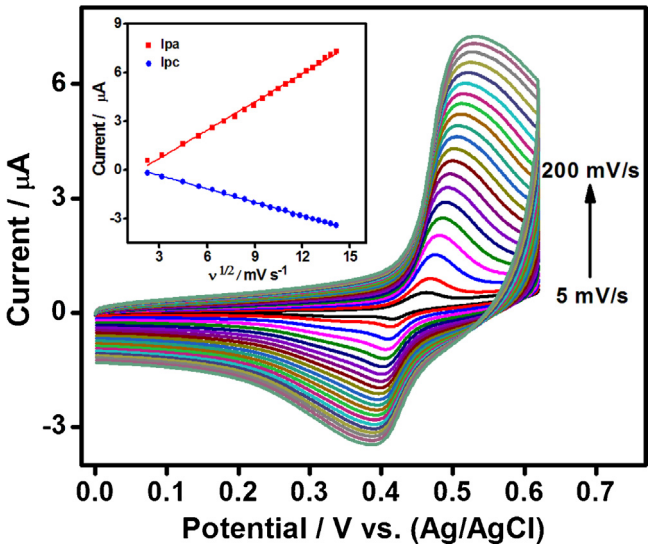

Fig. 6. Cyclic voltammograms of NiO-TiO_2/GCE modified electrode in presence of 0.1 M NaOH at increasing scan rates from 5 mV s^{-1} to 200 mV s^{-1}. The corresponding anodic peak current and cathodic peak current as a function of square root of the scan rate are shown in the inset.

To examine the nature of electrochemical process at the electrode surface, NiO-TiO_2/GC electrode was subjected to CV at a different scan rates ranging from 5 mV s^{-1} to 200 mV s^{-1} as presented in Fig. 6. Both anodic and cathodic peak currents increase as a scan rate increases revealing that the redox behavior of NiO-TiO_2/GCE possesses a linear relationship with square root of scan rate (Fig. 6 (inset)), which suggests a diffusion-confined electrochemical process. The above finding signifies the role of $Ni^{2+/3+}$ ions on the mixed oxide and show NiO-TiO_2 possesses excellent properties for the electrocatalytic oxidation of glucose.

3.2. Non-enzymatic electrocatalytic oxidation and amperometric determination of glucose

To determine the non-enzymatic glucose oxidation at different modified electrodes, CVs were recorded at bare GCE, TiO_2/GCE, NiO/GCE and NiO-TiO_2/GCE in presence of 1 mM glucose containing 0.1 M NaOH at a scan rate of 50 mV s^{-1}. As shown in Fig. 7a, bare GCE and TiO_2/GCE did not show any significant catalytic response for glucose oxidation when the potential sweep was performed within the potential range from 0 V to + 0.62 V. On the other hand, NiO/GCE exhibited significant enhancement in anodic peak current intensity confirming the glucose oxidation. The anodic peak current intensity further increased drastically along with a shift in anodic peak potential for NiO-TiO_2/GCE at the same glucose concentration confirming the mediator behavior of Ni^{2+}/Ni^{3+} redox couple. The drastic enhancement in glucose oxidation at Epa = 0.5 V with higher anodic peak current is attributed to the involvement of NiOOH. Therefore the electrocatalytic mechanism can be further explained as follows: Ni^{2+} is electrochemically oxidized to Ni^{3+} in presence of NaOH, followed by the oxidation of glucose to glucolactone by Ni^{3+} which is further reduced to Ni^{2+} at the electrode surface [44,45]. The anodic peak current response at NiO-TiO_2/GCE shows greater enhancement of about 2.3 fold than that of NiO/GCE which is attributed to the defect-induced mesoporous surface along with large surface area resulting to more effective glucose oxidation. Although the pristine TiO_2 possess large surface area, the absence of redox active sites leads to the no catalytic activity of glucose. Based on the high performance of NiO-TiO_2/GCE, we further explored the electrocatalytic behavior of this material at different glucose concentrations.

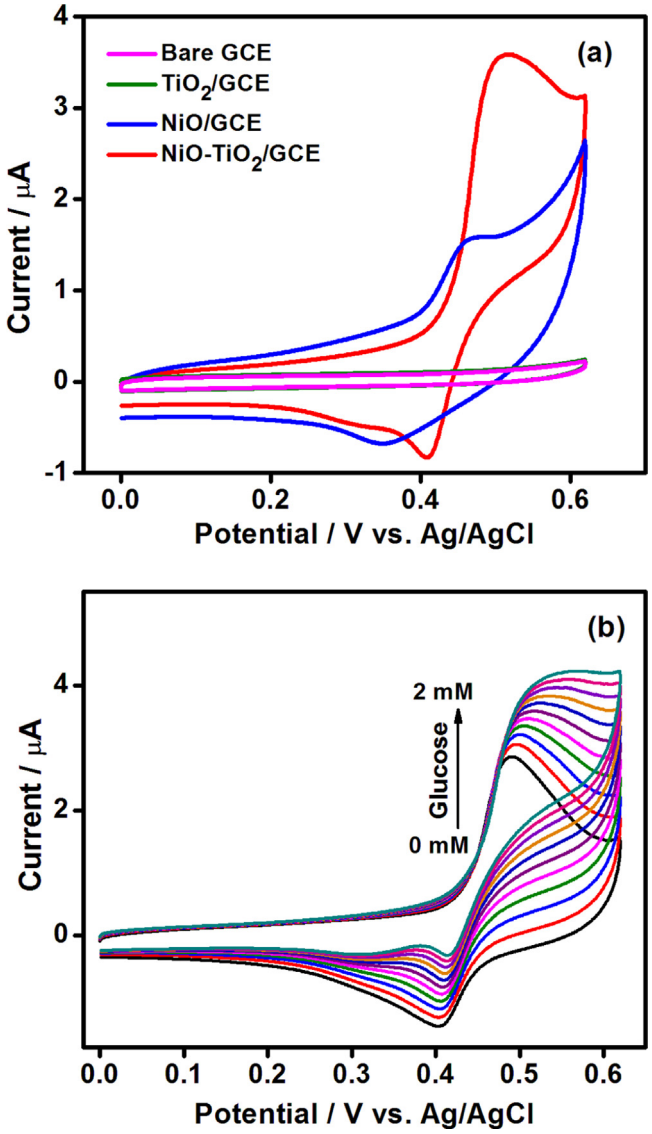

Fig. 7. (a) CVs of different modified electrodes namely bare GCE, TiO_2/GCE, NiO/GCE and NiO-TiO_2/GCE in presence of 1 mM glucose containing 0.1 M NaOH. (b) CV responses for NiO-TiO_2/GCE for successive addition of 0.2 mM glucose in presence of 0.1 M NaOH. Scan rate: 50 mV s^{-1}.

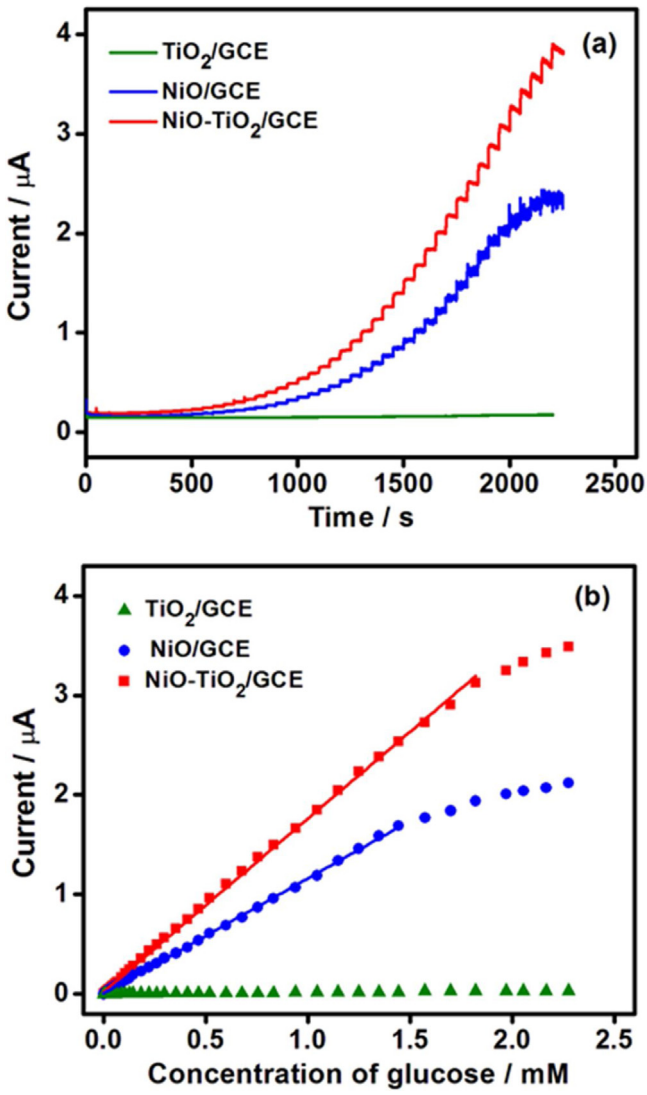

Fig. 8. (a) Amperometric responses for TiO_2/GCE, NiO/GCE and NiO-TiO_2/GCE upon successive addition of glucose to a stirring solution containing 0.1 M NaOH. Applied Potential: 0.5 V. (b) The corresponding calibration plot for the determination of glucose.

Fig. 7b depicts the electrocatalytic oxidation of glucose upon successive additions of 0.2 mM glucose in presence of 0.1 M NaOH. It can be observed that the anodic peak current of NiO-TiO_2/GCE increases gradually upon every addition of glucose demonstrating the electrocatalytic oxidation of glucose. Interestingly, the anodic peak current increased linearly with increase in concentration of the glucose which inspired us to develop an amperometric sensor for determination of glucose.

To evaluate the analytical performance of enzyme free glucose sensors, amperometric measurements were carried out at TiO_2/GCE, NiO/GCE and NiO-TiO_2/GCE with increasing concentration of glucose towards electrochemical oxidation of glucose. By holding the operating potential at 0.5 V, the amperometric response of the modified electrode (Fig. 8a) was monitored at 50 s intervals by addition of glucose into a stirring solution containing 0.1 M NaOH. The amperometric behavior of NiO-TiO_2/GCE shows a step-wise and rapid increase in oxidation current in comparison with NiO/GCE and TiO_2/GCE upon each addition of glucose and attained 95% of well-defined steady state current within 3 s. This rapid increase in the oxidation current response observed at NiO-TiO_2/GCE can be attributed to the mesoporous network of NiO interfacing with TiO_2 nanostructures and the presence of linear defects in nanostructured NiO-TiO_2. The calibration curve of glucose sensor (Fig. 8b) shows a linear dependence on glucose concentration in the range from 2 μM to 2 mM. The detection limit and sensitivity for NiO-TiO_2/GCE modified electrode were calculated as 0.7 μM (S/N = 3) and 24.85 μA mM^{-1} cm^{-2}, respectively. The obtained operating potential, linear range, sensitivity and detection limit values are comparable with or better than those of the reported NiO and TiO_2 based non-enzymatic glucose sensors (Table 1).

3.3. Non-enzymatic stability, reproducibility and anti-interference studies

The operational stability of the modified electrode was evaluated by recording CVs for 50 consecutive cycles at NiO-TiO_2/GCE within the potential range from 0 to 0.62 V in presence of 0.1 M NaOH at a scan rate of 50 mV s^{-1}. As shown in Fig. 9a, the modified electrode exhibits an extraordinary stability with no obvious change in redox peak current or potential. Therefore, the proposed

Table 1
Electrochemical performance of various non-enzymatic glucose sensors.

Electrodes	Potential (V)	Linear Range	Sensitivity	LOD (μM)	Ref.
Ti/TiO_2 nanotube array/Ni	0.55	10–110 μM	200 μA mM^{-1} cm^{-2}	4	[46]
Cu_2O/TiO_2 nanotube array	0.65	3.0–9.0 mM	14.56 μA mM^{-1} cm^{-2}	62	[19]
CuO/TiO2	0.5	up to 2.0 mM	79.79 μA mM^{-1} cm^{-2}	1	[20]
3D-KSCs/ZnO-NiO	0.5	0.013–4.86 mM	448.6 μA mM^{-1} cm^{-2}	4.12	[47]
Ag@NiO NWs/GCE	0.6	Up to 1.28 mM	67.51 μA mM^{-1} cm^{-2}	1.01	[48]
Ag&Pt-TiO_2	–	30–180 mM	3.99 μA mM^{-1} cm^{-2}	22.6	[49]
Cu-Cu_2O/TiO_2	0.65	0.1–2.5 mM	4895 μA mM^{-1} cm^{-2}	8.6	[50]
NiO-TiO_2	0.52	0.005–12.1	252 μA mM^{-1} cm^{-2}	1.0	[51]
$Ni/NiTiO_3/TiO_2$ nanotube	0.4	0.005–0.5	438.4 μA mM^{-1} cm^{-2}	0.7	[52]
Ti@TiO_2/Ni	0.55	0.005–9	114.0 μA mM^{-1} cm^{-2}	1	[53]
NiO/C-Ti	0.41	0.002–2.6 mM	582.6 μA mM^{-1} cm^{-2}	2	[54]
$Ni(OH)_2/TiO_xC_y$	0.7	0.02–1.7	120 μA mM^{-1}	5	[53]
NiO-TiO_2/GCE	0.5	0.002–2.0 mM	24.85 μA mM^{-1} cm^{-2}	0.7	This work

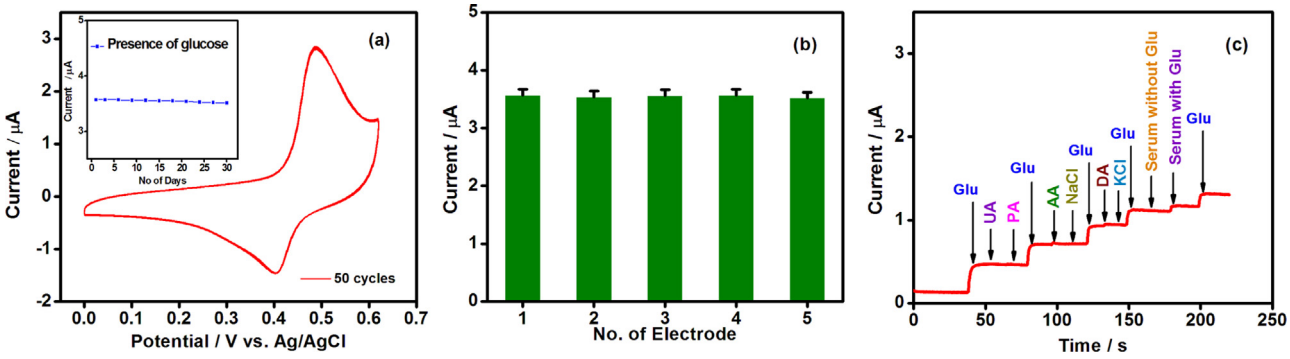

Fig. 9. (a) Cyclic voltammograms of NiO-TiO_2/GCE for continuous 50 cycles in presence of 0.1 M NaOH at a scan rate of 50 mV s^{-1}. The plot of day-day response for NiO-TiO_2/GCE in presence of 1 mM glucose is shown in inset. (b) The behavior of reproducibility for five different NiO-TiO_2/GCE. (c) Amperometric response for determination of interference species namely uric acid (UA), paracetamol (PA), ascorbic acid (AA), dopamine (DA), NaCl, KCl and serum at NiO-TiO_2/GCE in presence of 0.1 M glucose (Glu) under stirring 0.1 M NaOH. Applied potential: 0.5 V.

NiO-TiO_2/GCE revealed good operational stability. Furthermore, long-term stability of NiO-TiO_2/GCE was examined by measuring the response of modified electrode in presence of 1 mM glucose over the period of 30 days at each interval of 3 days. As observed from Fig. 9a. (Inset), NiO-TiO_2/GCE retained its electrochemical response in presence of glucose for 6 days and reached 94% of its response at the end of 30 days, exhibiting long-term stability. The electrochemical results obtained in this study indicate that our promising strategy to create defects on the TiO_2 nanoparticles and the formation of Ni^{3+} ions in the matrix synergistically improved the chemical stability of the modified electrode in basic solution. The unique structure of as-prepared NiO-TiO_2 shields the NiO from agglomeration, deformation of particles from electrode surface and breakdown of structure integrity over the longer period of time, demonstrating the prolonged glucose oxidation. To evaluate the reproducibility of modified electrode, five different NiO-TiO_2/GCE electrodes were fabricated independently under the same conditions and their electrocatalytic oxidation was examined in presence of 1 mM glucose (Fig. 9b). A relative standard deviation (R.S.D) of 2.4% was obtained, demonstrating a good reproducibility of NiO-TiO_2/GCE modified electrode.

Eliminating the possible interference species during selective oxidation of glucose is one of the major challenges in the development of successful electrochemical glucose sensors. The selectivity of NiO-TiO_2/GCE was investigated using amperometry by adding several oxidizable species such as uric acid, paracetamol, ascorbic acid, dopamine and chloride ions (i.e., from NaCl and KCl) into a 0.1 M NaOH solution containing glucose. It can be seen from Fig. 9c. that the amperometric response is negligible or shows no change in the anodic current response by adding an aliquot of 0.5 mM of each interferent species such as uric acid, paracetamol, ascorbic acid, dopamine, NaCl, KCl and 40 μM glucose free serum samples. It is well known that normal blood glucose level in humans is in the range between 4 mM and 7 mM, which is at least ten times higher than the concentrations of these interference species; therefore these feeble current response can be considered as negligible. Irrespective of interference species or their concentrations in the NaOH solution, a rapid increase in anodic current obtained by adding 0.1 mM glucose into the solution suggests that the foreign species did not alter the glucose oxidation even at higher concentrations used. These results show that NiO-TiO_2/GCE exhibits good selectivity and promising properties for determination of glucose in real samples.

Subsequently, NiO-TiO_2/GCE modified electrode was utilized for determination of glucose in human serum samples by implementing standard addition method. The human serum samples with the known glucose concentration of 5.1 mM were obtained from hospitalized patients. From the as-obtained serum samples, 1 mL of sample was diluted by adding 9 mL of 0.1 M NaOH followed by spiking of 0.5 and 1 mM known glucose concentration into the diluted solution. The amperometric experiments were carried out to investigate the glucose oxidation at NiO-TiO_2/GCE modified electrode. The concentration of the glucose in the human serum was determined and the values agreed well with the amperometric standard calibration curve. Each measurement was repeated three times and the RSD value was found to be less than 3% indicating the good precision of the proposed modified electrode. As seen in Table. 2, the obtained recovery values for the modified electrode are in the range from 98.6% to 99.3%. Hence, the proposed NiO-TiO_2/GCE modified

Table 2
Analysis of glucose in human serum.

Sample	Spiked (mM)	Found (mM)	Recovery (%)	RSD[a] (%)
Human	0	0.50	–	–
Serum	0.50	0.986	98.6	2.78
	1.50	1.490	99.3	2.62

[a] Three replicates were performed.

electrode provides a good platform for accurate determination of glucose in real samples.

4. Conclusion

This study introduces the defect-induced NiO-TiO_2 mixed oxide nanoparticles comprising Ni^{3+} ions for the selective detection of glucose. The outperformed electrochemical results indicate that our promising strategy generates defect on TiO_2 nanoparticles with the formation of Ni^{3+} ions in the matrix, which makes synergistic improvement in the sensitivity, response time, selectivity, reliability, and durability of the modified electrode in basic solution. This study demonstrates the detection limit and sensitivity for NiO-TiO_2/GCE modified electrode were about 0.7 μM (S/N = 3) and 24.85 $\mu A\,mM^{-1}\,cm^{-2}$, respectively. The analytical application of NiO-TiO_2/GCE towards the determination of human serum samples has been successfully demonstrated and the obtained recovery values are in the range between 98.6 to 99.3%. Thus our finding is certainly beneficial to broaden the perspective of glucose biosensing applications.

Conflict of interest

The authors declare that there is no regarding the publication of this article.

Acknowledgements

The authors (S.R., F.G.) acknowledge the support of CONICYT through the project CONICYT/FONDAP/15110019. The authors (M. Naushad and T. Ahamad) would like to extend their sincere appreciation to the Deanship of Scientific Research at King Saud University for funding this work through Research Group No. (RG-1436-034).

Appendix A. Supplementary data

Supplementary data associated with this article can be found, in the online version, at https://doi.org/10.1016/j.snb.2018.02.165.

References

[1] E. Witkowska Nery, M. Kundys, P.S. Jeleń, M. Jönsson-Niedziółka, Electrochemical glucose sensing: is there still room for improvement? Anal. Chem. 88 (2016) 11271–11282, http://dx.doi.org/10.1021/acs.analchem.6b03151.
[2] Wild Sarah, Roglic Gojka, Green Anders, Sicree Richard, K. Hilary, Global prevalence of diabetes: estimates for theyear 2000 and projection for 2030, Diabetes Care 27 (2004) 1047–1053, http://dx.doi.org/10.2337/diacare.27.5.1047.
[3] J. Wang, Electrochemical glucose biosensors, Chem. Rev. 108 (2008) 814–825, http://dx.doi.org/10.1021/cr068123a.
[4] A.P.F. Turner, Biosensors: sense and sensibility, Chem. Soc. Rev. 42 (2013) 3184–3196, http://dx.doi.org/10.1039/c3cs35528d.
[5] R. Gifford, Continuous glucose monitoring: 40 years, what we've learned and what's next, ChemPhysChem 14 (2013) 2032–2044, http://dx.doi.org/10.1002/cphc.201300172.
[6] A. Heller, B. Feldman, Electrochemical glucose sensors and their applications in diabetes management, Chem. Rev. 108 (2008) 2482–2505, http://dx.doi.org/10.1021/cr068069y.
[7] K.E. Toghill, R.G. Compton, Electrochemical non-enzymatic glucose sensors: a perspective and an evaluation, Int. J. Electrochem. Sci. 5 (2010) 1246–1301, http://dx.doi.org/10.1016/j.ccr.2016.04.01.
[8] S. Palanisamy, S.M. Chen, R. Sarawathi, A novel nonenzymatic hydrogen peroxide sensor based on reduced graphene oxide/ZnO composite modified electrode, Sens. Actuators B Chem. 166–167 (2012) 372–377, http://dx.doi.org/10.1016/j.snb.2012.02.075.
[9] P. Si, Y. Huang, T. Wang, J. Ma, Nanomaterials for electrochemical non-enzymatic glucose biosensors, RSC Adv. 3 (2013) 3487, http://dx.doi.org/10.1039/c2ra22360k.
[10] M. Benjamin, D. Manoj, K. Thenmozhi, P.R. Bhagat, D. Saravanakumar, S. Senthilkumar, A bioinspired ionic liquid tagged cobalt-salophen complex for nonenzymatic detection of glucose, Biosens. Bioelectron. 91 (2017) 380–387, http://dx.doi.org/10.1016/j.bios.2016.12.064.
[11] J. Schneider, M. Matsuoka, M. Takeuchi, J. Zhang, Y. Horiuchi, M. Anpo, D.W. Bahnemann, Understanding TiO_2 photocatalysis: mechanisms and materials, Chem. Rev. 114 (2014) 9919–9986, http://dx.doi.org/10.1021/cr5001892.
[12] Peng Si, S. Ding, J. Yuan, X. (David) Lou, D.-H. Kim, Hierarchically structured one- dimensional TiO_2 for protein immobilization, direct electrochemistry, and mediator- free glucose sensing, ACS Nano 5 (2011) 7617–7626, http://dx.doi.org/10.1021/nn202714c.
[13] J. Liu, Z. He, S.Y. Khoo, T.T.Y. Tan, A new strategy for achieving vertically-erected and hierarchical TiO_2 nanosheets array/carbon cloth as a binder-free electrode for protein impregnation, direct electrochemistry and mediator-free glucose sensing, Biosens. Bioelectron. 77 (2016) 942–949, http://dx.doi.org/10.1016/j.bios.2015.10.070.
[14] Q. Li, G. Luo, J. Feng, Q. Zhou, L. Zhang, Y. Zhu, Amperometric detection of glucose with glucose oxidase absorbed on porous nanocrystalline TiO_2 film, Electroanalysis 13 (2001) 413–416 (1040-0397/01/0504±0413).
[15] J. Cai, J. Huang, M. Ge, J. Iocozzia, Z. Lin, K.-Q. Zhang, Y. Lai, Immobilization of Pt nanoparticles via rapid and reusable electropolymerization of dopamine on TiO_2 nanotube arrays for reversible SERS substrates and nonenzymatic glucose sensors, Small 13 (2017), http://dx.doi.org/10.1002/smll.201604240.
[16] L. Wang, X. Lu, C. Wen, Y. Xie, L. Miao, S. Chen, H. Li, P. Li, Y. Song, One-step synthesis of Pt–NiO nanoplate array/reduced graphene oxide nanocomposites for nonenzymatic glucose sensing, J. Mater. Chem. 3 (2015) 608–616, http://dx.doi.org/10.1039/C4TA04724A.
[17] S. Sun, Y. Sun, A. Chen, X. Zhang, Z. Yang, Nanoporous copper oxide ribbon assembly of free-standing nanoneedles as biosensors for glucose, Analyst 140 (2015) 5205–5215, http://dx.doi.org/10.1039/C5AN00609K.
[18] R. Madhu, V. Veeramani, S.M. Chen, A. Manikandan, A.Y. Lo, Y.L. Chueh, Honeycomb-like porous carbon-cobalt oxide nanocomposite for high-performance enzymeless glucose sensor and supercapacitor applications, ACS Appl. Mater. Interfaces 7 (2015) 15812–15820, http://dx.doi.org/10.1021/acsami.5b04132.
[19] M. Long, L. Tan, H. Liu, Z. He, A. Tang, Novel helical TiO_2 nanotube arrays modified by Cu2O for enzyme-free glucose oxidation, Biosens. Bioelectron. 59 (2014) 243–250, http://dx.doi.org/10.1016/j.bios.2014.03.032.
[20] S. Luo, F. Su, C. Liu, J. Li, R. Liu, Y. Xiao, Y. Li, X. Liu, Q. Cai, A new method for fabricating a CuO/TiO_2 nanotube arrays electrode and its application as a sensitive nonenzymatic glucose sensor, Talanta 86 (2011) 157–163, http://dx.doi.org/10.1016/j.talanta.2011.08.051.
[21] Q. Yang, M. Long, L. Tan, Y. Zhang, J. Ouyang, P. Liu, A. Tang, Helical TiO_2 nanotube arrays modified by Cu-Cu_2O with ultrahigh sensitivity for the nonenzymatic electro-oxidation of glucose, ACS Appl Mater. Interfaces 7 (2015) 12719–12730, http://dx.doi.org/10.1021/acsami.5b03401.
[22] P.V. Suneesh, V. Sara Vargis, T. Ramachandran, B.G. Nair, T.G. Satheesh Babu, Co–Cu alloy nanoparticles decorated TiO_2 nanotube arrays for highly sensitive and selective nonenzymatic sensing of glucose, Sens. Actuators B Chem. 215 (2015) 337–344, http://dx.doi.org/10.1016/j.snb.2015.03.073.
[23] C. Guo, H. Huo, X. Han, C. Xu, H. Li, Ni/CdS bifunctional Ti@TiO_2 core-shell nanowire electrode for high-performance nonenzymatic glucose sensing, Anal. Chem. 86 (2014) 876–883, http://dx.doi.org/10.1021/ac4034467.
[24] Y. Zhang, Y. Wang, J. Jia, J. Wang, Nonenzymatic glucose sensor based on graphene oxide and electrospun NiO nanofibers, Sens. Actuators B Chem. 171–172 (2012) 580–587, http://dx.doi.org/10.1016/j.snb.2012.05.037.
[25] P. Yang, X. Tong, G. Wang, Z. Gao, X. Guo, Y. Qin, NiO/SiC nanocomposite prepared by atomic layer deposition used as a novel electrocatalyst for nonenzymatic glucose sensing, ACS Appl. Mater. Interfaces 7 (2015) 4772–4777, http://dx.doi.org/10.1021/am508508m.
[26] Z. Da Gao, Y. Han, Y. Wang, J. Xu, Y.Y. Ong, One-step to prepare self-organized nanoporous NiO/TiO_2 layers and its use in non-enzymatic glucose sensing, Sci. Rep. 3 (2013), http://dx.doi.org/10.1038/srep03323.
[27] Z.W. Pan, Nanobelts of semiconducting oxides, Science 291 (2001) 1947–1949, http://dx.doi.org/10.1126/science.1058120.
[28] L.G. Devi, N. Kottam, B.N. Murthy, S.G. Kumar, Enhanced photocatalytic activity of transition metal ions Mn^{2+}, Ni^{2+} and Zn^{2+} doped polycrystalline titania for the degradation of Aniline Blue under UV/solar light, J. Mol. Catal. A Chem. 328 (2010) 44–52, http://dx.doi.org/10.1016/j.molcata.2010.05.021.
[29] C. Karunakaran, A. Ganapathy, G. Paramasivan, M. Govindasamy, A. Viswanathan, NiO/TiO_2 nanoparticles for photocatalytic disinfection of bacteria under visible light, J. Am. Ceram. Soc. (2011) 2499–2505.
[30] L. Li, B. Cheng, Y. Wang, J. Yu, Enhanced photocatalytic H_2-production activity of bicomponent NiO/TiO_2 composite nanofibers, J. Colloid Interface Sci. 449 (2015) 115–121, http://dx.doi.org/10.1016/j.jcis.2014.10.072.
[31] N.K. Shrestha, M. Yang, Y.C. Nah, I. Paramasivam, P. Schmuki, Self-organized TiO_2 nanotubes: visible light activation by Ni oxide nanoparticle decoration, Electrochem. Commun. 12 (2010) 254–257, http://dx.doi.org/10.1016/j.elecom.2009.12.007.

[32] D. Wang, Z.-H. Zhou, H. Yang, K.-B. Shen, Y. Huang, S. Shen, Preparation of TiO_2 loaded with crystalline nano Ag by a one-step low-temperature hydrothermal method, J. Mater. Chem. 22 (2012) 16306, http://dx.doi.org/10.1039/c2jm16217b.
[33] X. Wang, T.T. Lim, Highly efficient and stable Ag-AgBr/TiO_2 composites for destruction of Escherichia coli under visible light irradiation, Water Res. 47 (2013) 4148–4158, http://dx.doi.org/10.1016/j.watres.2012.11.057.
[34] S. Wang, H. Qian, Y. Hu, W. Dai, Y. Zhong, J. Chen, X. Hu, Facile one-pot synthesis of uniform TiO_2–Ag hybrid hollow spheres with enhanced photocatalytic activity, Dalton Trans. 42 (2013) 1122–1128, http://dx.doi.org/10.1039/C2DT32040A.
[35] K. Sivaranjani, C.S. Gopinath, Porosity driven photocatalytic activity of wormhole mesoporous $TiO_{2-x}N_x$ in direct sunlight, J. Mater. Chem. 21 (2011) 2639, http://dx.doi.org/10.1039/c0jm03825c.
[36] R. Peng, K. Shrestha, G. Mishra, J. Baltrusaitis, C.-M. Wu, R.T. Koodali, Efficient photocatalytic hydrogen evolution system by assembling earth abundant Ni_xO_y nanoclusters in cubic MCM-48 mesoporous materials, RSC Adv. 6 (2016) 59169–59180, http://dx.doi.org/10.1039/C6RA09126A.
[37] A. Folger, P. Ebbinghaus, A. Erbe, C. Scheu, Role of vacancy condensation in the formation of voids in rutile TiO_2 nanowires, ACS Appl. Mater. Interfaces 9 (2017) 13471–13479, http://dx.doi.org/10.1021/acsami.7b01160.
[38] B.J. Morgan, G.W. Watson, Intrinsic n-type defect formation in TiO_2: a comparison of rutile and anatase from GGA + U calculations, J. Phys. Chem. C 114 (2010) 2321–2328, http://dx.doi.org/10.1021/jp9088047.
[39] Y. Wang, Y. Su, M. Zhu, L. Kang, Ni cluster nucleation and growth on the anatase TiO_2 (101) surface: a density functional theory study, RSC Adv. 5 (2015) 16582–16591, http://dx.doi.org/10.1039/C4RA13975E.
[40] J. Nowotny, M.A. Alim, T. Bak, M.A. Idris, M. Ionescu, K. Prince, M.Z. Sahdan, K. Sopian, M.A. Mat Teridi, W. Sigmund, Defect chemistry and defect engineering of TiO_2 –based semiconductors for solar energy conversion, Chem. Soc. Rev. 44 (2015) 8424–8442, http://dx.doi.org/10.1039/C4CS00469H.
[41] J. Lin, J. Shen, R. Wang, J. Cui, W. Zhou, P. Hu, D. Liu, H. Liu, J. Wang, R.I. Boughton, Y. Yue, Nano-p–n junctions on surface-coarsened TiO_2 nanobelts with enhanced photocatalytic activity, J. Mater. Chem. 21 (2011) 5106, http://dx.doi.org/10.1039/c0jm04131a.
[42] J.D. Bass, C. Boissiere, L. Nicole, D. Grosso, C. Sanchez, Thermally induced porosity in CSD MgF_2-based optical coatings: an easy method to tune the refractive index, Chem. Mater. 20 (2008) 5550–5556, http://dx.doi.org/10.1021/cm8010106.
[43] C. Rodriguez-Navarro, E. Ruiz-Agudo, A. Luque, A.B. Rodriguez-Navarro, M. Ortega-Huertas, Thermal decomposition of calcite: mechanisms of formation and textural evolution of CaO nanocrystals, Am. Mineral. 94 (2009) 578–593, http://dx.doi.org/10.2138/am.2009.3021.
[44] X. Niu, M. Lan, H. Zhao, C. Chen, Highly sensitive and selective nonenzymatic detection of glucose using three-dimensional porous nickel nanostructures, Anal. Chem. 85 (2013) 3561–3569, http://dx.doi.org/10.1021/ac3030976.
[45] T. Chen, D. Liu, W. Lu, K. Wang, G. Du, A.M. Asiri, X. Sun, Three-dimensional Ni2P nanoarray: an efficient catalyst electrode for sensitive and selective nonenzymatic glucose sensing with high specificity, Anal. Chem. 88 (2016) 7885–7889, http://dx.doi.org/10.1021/acs.analchem.6b02216.
[46] C. Wang, L. Yin, L. Zhang, R. Gao, Ti/TiO_2 nanotube Array/Ni composite electrodes for nonenzymatic amperometric glucose sensing, J. Phys. Chem. 114 (2010) 4408–4413, http://dx.doi.org/10.1021/jp912232p.
[47] Y. Zhang, L. Wang, J. Yu, H. Yang, G. Pan, L. Miao, Y. Song, Three-dimensional macroporous carbon supported hierarchical ZnO-NiO nanosheets for electrochemical glucose sensing, J. Alloys Compd. 698 (2017) 800–806, http://dx.doi.org/10.1016/j.jallcom.2016.12.276.
[48] J. Song, L. Xu, R. Xing, W. Qin, Q. Dai, H. Song, Ag nanoparticles coated NiO nanowires hierarchical nanocomposites electrode for nonenzymatic glucose biosensing, Sens. Actuators B Chem. 182 (2013) 675–681, http://dx.doi.org/10.1016/j.snb.2013.03.069.
[49] X. Wang, X. Xia, X. Zhang, W. Meng, C. Yuan, M. Guo, Nonenzymatic glucose sensor based on Ag&Pt hollow nanoparticles supported on TiO_2 nanotubes, Mater. Sci. Eng. C 80 (2017) 174–179, http://dx.doi.org/10.1016/j.msec.2017.05.137.
[50] Q. Yang, M. Long, L. Tan, Y. Zhang, J. Ouyang, P. Liu, A. Tang, Helical TiO_2 nanotube arrays modified by Cu-Cu_2O with ultrahigh sensitivity for the nonenzymatic electro-oxidation of glucose, ACS Appl. Mater. Interfaces 7 (2015) 12719–12730, http://dx.doi.org/10.1021/acsami.5b03401.
[51] Z.-D. Gao, Y. Han, Y. Wang, J. Xu, Y.-Y. Song, One-step to prepare self-organized nanoporous NiO/TiO_2 Layers and its use in non-enzymatic glucose sensing, Sci. Rep. 3 (2013) 3323, http://dx.doi.org/10.1038/srep03323.
[52] K. Huo, Y. Li, R. Chen, B. Gao, C. Peng, W. Zhang, L. Hu, X. Zhang, P.K. Chu, Recyclable non-enzymatic glucose sensor based on Ni/$NiTiO_3$/TiO_2 nanotube arrays, ChemPlusChem 80 (2015) 576–582, http://dx.doi.org/10.1002/cplu.201402288.
[53] C. Guo, H. Huo, X. Han, C. Xu, H. Li, Ni/CdS bifunctional Ti@TiO_2 core-shell nanowire electrode for high performance nonenzymatic glucose sensing, Anal. Chem. 86 (2014) 876–883, http://dx.doi.org/10.1021/ac4034467.
[54] X. Li, A. Hu, J. Jiang, R. Ding, J. Liu, X. Huang, Preparation of nickel oxide and carbon nanosheet array and its application in glucose sensing, J. Solid State Chem. 184 (2011) 2738–2743, http://dx.doi.org/10.1016/j.jssc.2011.08.008.

Biographies

Dr Saravanan Rajendran received his postgraduate studies in Thiruvalluvar University (Sacred Heart College), India during the year of 2005–2007 and was awarded first class with University rank. He has completed his M.Phil and Ph.D in Physics (Material Science), in the Department of Nuclear Physics, University of Madras, India with first class and highly recommended thesis by the reviewers. He was awarded University Research Fellowship (URF) during the year 2009–2011 by the University of Madras. After working as an Assistant Professor in Dhanalakshmi College of Engineering, Chennai, India during the year of 2013–2014. He was awarded SERC and CONICYT-FONDECYT post-doctoral fellowship, University of Chile, Santiago-Chile in the year of 2014. He has published several International peer-reviewed Journals and including a book chapter. His work interest includes Nanoporous and Nanomaterials based catalysts for renewable energy and waste water purification.

Dr Manoj Devaraj received a PhD degree in Physical Chemistry from the University of Madras, India. After completed his Ph.D. he acquired his postdoctoral position under Prof. Nurit Ashkenasy, at Department of Materials Engineering, Ben-Gurion University, Israel and currently working as postdoctoral fellowship in VIT University, India. His recent research interests has been focused on design and development of various nanostructured materials, ionic liquids and carbon materials as electrode materials for electrochemical biosensors and energy applications.

Dr Kumar Raju received a PhD degree in Chemistry (Chemistry – Energy interdisciplinary) from the University of Madras, India. He was awarded Junior and Senior research fellowships from DST and CSIR, India during his PhD tenure and then he was joined as Postdoctoral Fellow (2012) in Hanyang University, South Korea. He then joined the Council for Scientific and Industrial Research (CSIR), South Africa in 2013 as Postdoctoral Fellow, he is currently a Senior Researcher at the CSIR. He has 25 peer-reviewed articles and 2 patents to his credit. His research interest focusses on electrochemical materials science and developing advanced materials for energy storage and conversions.

Dr. Dionysios (Dion) D. Dionysiou is currently a Professor of Environmental Engineering and Science Program at the University of Cincinnati. He teaches courses and performs research in the areas of water quality, treatment, and monitoring. He is the author or co-author of over 350 refereed journal publications and his work received over 23,000 citations with an H factor of 79. Web Page 1: http://ceas.uc.edu/chemical-environmental-engineering/Dr_Dion_lab.html Web Page 2: http://ceas.uc.edu/chemical-environmental-engineering/Dr_Dionysios_Dionysiou.html. Professor Dionysiou is currently a UNESCO co-Chair Professor on "Water Access and Sustainability" and a Herman Schneider Professor of Environmental Engineering at the University of Cincinnati. He teaches courses on drinking water quality, treatment and reuse, advanced unit operations for water treatment, advanced oxidation technologies, and physical-chemical processes for water quality control. Professor Dionysiou is leading several projects of local, state, national and international importance focused on water quality, treatment, reuse, and monitoring. His work encompasses surface water, groundwater, agricultural water, and industrial waters of complex mixtures. His research interests include (i) physical chemical processes for water treatment, (ii) urban water quality, (iii) advanced oxidation processes, (iv) UV and solar light-based remediation processes, (v) treatment of contaminants of emerging concern (i.e., pharmaceuticals and personal care products, biotoxins, heavy metals), (vi) remediation of Harmful Algal Blooms/cyanotoxins, (vii) environmental nanotechnology and nanosensing, (viii) water-energy-food (WEF) nexus, and (ix) water sustainability. Several of his current projects are focused on the treatment, sensing and monitoring of cyanotoxins formed in freshwater aquatic systems such as Lake Erie and several inland lakes and rivers in Ohio.

Dr. Mu. Naushad is an Associate Professor in the Department of Chemistry, College of Science, King Saud University (KSU), Saudi Arabia. He received his Ph.D Degree in Analytical chemistry, from A.M.U. Aligarh, India in 2007. His research interest includes nanocomposite materials and wastewater treatment. He has over 200 refereed publications with a Google Scholar H-Index of >35. He holds several US patents derived from his research. He is the Editor/Editorial member of several reputed Journals like Scientific Report (Nature) and Process Safety & Env. Protection (Elsevier). He has been awarded by the Scientist of the year award-2015 from National Environmental Science Academy, Delhi, India and Almarai Award-2017, Saudi Arabia.

Dr F. Gracia obtained his Ph.D degree at University of Notre Dame, USA, in 2004. For his research about the state of the catalytic surface on Pt supported catalysts he was awarded the Manly Award for Excellence in Materials Science. The same year he joined the Department of Chemical Engineering and Biotechnology at the University of Chile, where he currently is Associate Professor. He has published several International peer-reviewed Journals and responsible in more than 10 research projects with public and private funding. His work interest involves the Heterogeneous Catalysis area, focusing on Nanoporous and Nanomaterials based catalysts for renewable energy, H_2 production and CO_2 activation for SNG production.

Dr Lorena Cornejo is a laboratory chemist at the University of Chile and has a master's in chemistry with honorable mention in analytical chemistry from the University of Estadual de Campinas in Brazil. She also completed a post-doctoral degree in the same Brazilian university. She currently works as a professor at the University of Tarapacá. Her research is dedicated to the evaluation and distribution

of the chemical elements water and earth. She also investigates the development of technologies for decontaminating and disinfecting water.

Dr Gracia Pinilla, M.A obtained his B.S. degree with honor from National University of Colombia. Colombia and Ph.D. from Autonomous University of New Leon (2008). México and then performed a Sabbatical year at Florida International University (FIU) (2015), U.S.A. He has worked at Autonomous University of New Leon as an Associate professor from 2008. He Works on nanotechnology and its application to solar energy conversion and photocatalytic materials.

Dr. Tansir Ahamad is an Associate Professor in the Department of Chemistry, College of Science, King Saud University (KSU), Saudi Arabia. He received his Ph.D Degree in Materials Chemistry, from Jamia Millia Islamia, New Delhi, India in 2006. His research interest includes the fabrication of novel nanomaterials, hybrid materials and their industrial applications. He published more than 140 research papers in international journals and he has 8 US and 1 European patent issued. Additionally, several papers and patents are in process for publication.